

# Electro-optic sampling system with a single-crystal 4-N,N-dimethylamino-4'-N'-methyl-4-stilbazolium tosylate sensor

X. Zheng, S. Wu,<sup>a)</sup> and Roman Sobolewski<sup>b)</sup>

*Department of Electrical and Computer Engineering and the Laboratory for Laser Energetics, University of Rochester, Rochester New York 14627-0231*

R. Adam, M. Mikulics, and P. Kordoš

*Institute of Thin Films and Interfaces, Research Center Jülich, D-52425 Jülich, Germany*

M. Siegel

*Institut für Elektrotechnische Grundlagen der Informatik, Universität Karlsruhe, D-76187 Karlsruhe, Germany*

(Received 2 January 2003; accepted 9 February 2003)

We present an electro-optic (EO) sampling system based on an organic ionic salt crystal, 4-N,N-dimethylamino-4'-N'-methyl-4-stilbazolium tosylate (DAST) transducer. Compared to LiTaO<sub>3</sub>, the DAST lower dielectric permittivity and much higher electro-optic coefficient dramatically improve electric-field coupling into the EO crystal, which results in a much better signal-to-noise ratio of the sampling system. Submillivolt signals can be easily measured with the DAST sensor. Time resolution of the DAST-based EO system is the same as that of the LiTaO<sub>3</sub>-based sampler. © 2003 American Institute of Physics. [DOI: 10.1063/1.1565508]

The organic ionic salt crystal 4-N,N-dimethylamino-4'-N'-methyl-4-stilbazolium tosylate (DAST) is a very promising nonlinear optical (NLO) material. DAST has been demonstrated to have a very large NLO susceptibility and the largest electro-optic (EO) coefficient of all materials researched to date.<sup>1-5</sup> Originally designed for EO applications, the material has its charge-transfer axis of the stilbazolium chromophore deviating only 20° from the polar axis of the crystal, which is an arrangement well optimized for linear electro-optics. Like other organic crystals, the NLO effects in DAST originate from the extended  $\pi$ -electron system, so its response time is very short.<sup>6</sup> In addition, DAST has much lower values of the dielectric constants ( $\epsilon_a=5.2$ ,  $\epsilon_b=4.1$ , and  $\epsilon_c=3.0$ ) as compared to conventional inorganic EO materials such as LiTaO<sub>3</sub> ( $\epsilon_a=\epsilon_b=41$ ,  $\epsilon_c=43$ ), or LiNbO<sub>3</sub> ( $\epsilon_a=\epsilon_b=44$ ,  $\epsilon_c=29$ ). All of the above characteristics make DAST an ideal material for broadband EO applications, such as EO switches, modulators, or sensors.

Shortly after the first DAST single crystals were synthesized, many efforts were undertaken to implement this material to ultrafast optoelectronic systems. The most successful application of DAST was in the THz-frequency regime for generation and detection of free-space propagating THz pulses. Zhang *et al.* observed the THz radiation generated from DAST by optical rectification,<sup>7</sup> and, subsequently, other groups successfully generated THz pulses with center frequencies much higher than those obtained from inorganic THz emitters, such as ZnTe, LiTaO<sub>3</sub>, or LiNbO<sub>3</sub>.<sup>8-10</sup> Han *et al.* were the first to use DAST for THz radiation detection.<sup>11</sup> Subsequently, Litz *et al.* extended this technique

and proposed a DAST-based, wideband, electric field sensor,<sup>12</sup> intended to replace conventional metallic probes in high-frequency, high-electric-field testing. Other implementations of DAST single crystals include EO modulators,<sup>13,14</sup> gratings,<sup>15</sup> frequency doublers, and optic parametric oscillators in the near infrared.<sup>16-19</sup>

In this letter, we demonstrate the use of DAST in an EO sampling system<sup>20</sup> by measuring picosecond duration, submillivolt amplitude photoresponse transients, generated by femtosecond optical excitation of a metal-semiconductor-metal (MSM) diode. The diode was fabricated on a low-temperature (LT)-grown GaAs free-standing crystal and transferred onto a coplanar waveguide (CPW) on a MgO substrate.<sup>21</sup> We report on the DAST performance as an EO sensor by comparing it with the conventional LiTaO<sub>3</sub> sensor that has been used for EO sampling for the last two decades.<sup>20</sup>

The DAST sample used in our experiments was purchased from Rainbow Photonics.<sup>22</sup> It is a dark red, platelet-type single crystal with the following dimensions: 4.2, 1.6, and 0.295 mm along the *a*, *b*, and *c* crystallographic axes, respectively. The two optical surfaces have been polished to reach an optical flatness of about  $\lambda/4-\lambda/2$  ( $\lambda=632.8$  nm), measured by a polarizing microscope. DAST belongs to the monoclinic space group *Cc* (point group *m*, *z*=4). The angles between the dielectric axes  $x_1$  and  $x_3$  and the crystallographic axes *a* and *c* are 5.4° and 3.2°, respectively, whereas the  $x_2$  axis coincides with the *b* axis.<sup>5</sup> Designing our experiment, however, we ignored these small mismatch angles and assumed for simplicity that the dielectric and crystallographic axes coincided.

The schematics of our experimental setup is shown in Fig. 1. The excitation beam and the probe (sampling) beam were generated by the same commercial Ti:sapphire laser and consisted of trains of 100-fs-wide, 810-nm-wavelength

<sup>a)</sup>Also at: the Department of Physics and Astronomy, University of Rochester, Rochester, NY 14627.

<sup>b)</sup>Also at: the Institute of Physics, Polish Academy of Sciences, PL-02668 Warszawa, Poland; electronic mail: roman.sobolewski@rochester.edu

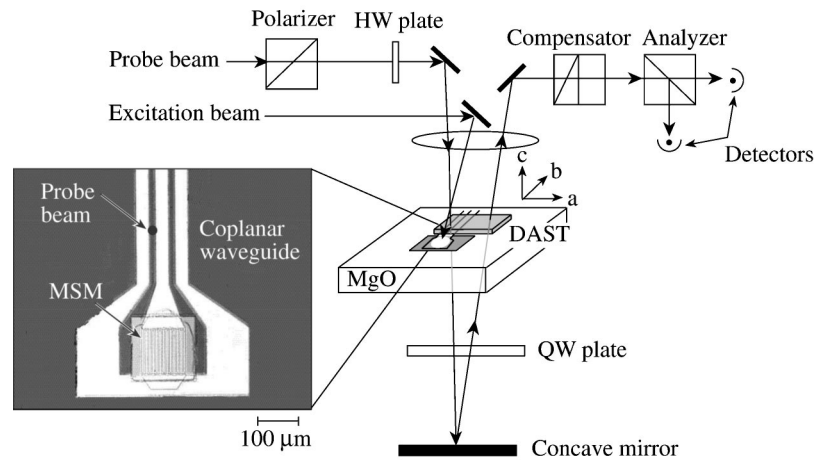


FIG. 1. Schematics of the EO sampling experiment using the DAST transducer. Note the orientation of the DAST crystal. The inset shows a micrograph of our test sample details. The MSM finger width was  $2\ \mu\text{m}$  and the finger spacing  $4\ \mu\text{m}$ .

pulses at an 82 MHz repetition rate. The excitation beam passed through a  $10\times$ , 50-mm-working-distance microscope objective and illuminated the MSM diode, shown in the inset in Fig. 1. The diode was patterned on a  $150 \times 150\ \mu\text{m}^2$  area, free-standing LT-GaAs crystal and incorporated into the Ti/Au CPW that interconnected the MSM diode. The entire structure was fabricated on a MgO substrate. Detailed discussion on characteristics and properties of free-standing LT-GaAs devices transferred onto various substrates have been given by us elsewhere.<sup>21,23</sup> The probe beam passed through a polarizer, a half-wave (HW) plate, and the same microscope objective as the excitation beam, before reaching the DAST crystal, which was overlaid on top of CPW. Next, the probe beam passed through the  $10\ \mu\text{m}$  gap in the CPW electrodes, and its spot size at the CPW gap was  $<10\ \mu\text{m}$  (see the inset in Fig. 1).

As shown in Fig. 1, the  $a$  axis of the DAST crystal (long edge) was oriented parallel to the electric field of the photoresponse transients propagating along the CPW. The HW plate was rotated such that the polarization of the probe beam entering DAST was  $45^\circ$  with respect to the crystal  $a$  axis. This arrangement gave us the highest EO modulation effect of DAST in the way of a polarimeter. To overcome the problem of losing coherence due to the huge static birefringence of DAST ( $n_a \approx 2.46$ ,  $n_b \approx 1.68$ , at the 805 nm wavelength), we implemented the transmission geometry, which was first used by Han *et al.*<sup>11</sup> in their study of DAST as a THz radiation detector. After the MgO substrate, the probe beam traveled through a quarter-wave (QW) plate, was reflected by a concave mirror (EFL=100 mm), and again passed through the QW plate and the DAST crystal. The fast axis of the QW plate was aligned  $45^\circ$  with respect to the  $a$  axis of the DAST crystal. Since the double pass through the QW plate is equivalent to a single pass of a HW plate, the initial  $a$  component of the probe-beam polarization was rotated by  $90^\circ$  to become a  $b$  component, and the initial  $b$  component became an  $a$  component. When the sampling beam went through the DAST crystal for the second time, its  $a$  component, which experienced  $n_a$  during the first time pass, experienced  $n_b$  for this time, and vice versa. Therefore, the effect of the DAST's static birefringence was canceled out. In other words, the use of the QW plate and the concave

mirror canceled out the effect of static birefringence in a way that was equivalent to using two identical DAST crystals that are rotated  $90^\circ$  with respect to each other (an arrangement frequently found in EO sensors exhibiting large static birefringence). The temporal separation of  $\sim 1.3\ \text{ns}$  between the first and the second transmission of the probe beam through the DAST crystal (determined by the beam total traveling distance of  $\sim 40\ \text{cm}$ ), together with the physical separation of the probe spots, guaranteed that during the second transmission through the DAST sensor, the probe beam would experience no polarization change due to the photoresponse signal we studied.

A second polarizer at the end of the probe-beam optical path was used as an analyzer to measure the polarization change that occurred during the first pass through the DAST crystal, due to the electrical transient generated by the photoexcited MSM diode. The compensator, placed before the analyzer, was used to optically set the  $\pi/2$  operation point on the EO sensor transform function, which corresponds to the linear operation regime. Finally, the probe signal was detected by a pair of balanced, 1-GHz-bandwidth, low-noise photoreceivers. A lock-in-based, differential mode of detection was implemented to eliminate the laser-amplitude-fluctuation noise and double the measured signal amplitude. The lock-in output signal (not shown in Fig. 1) was fed to a computer data acquisition system, where it was calibrated, averaged over a desired number of traces, and displayed on the monitor.

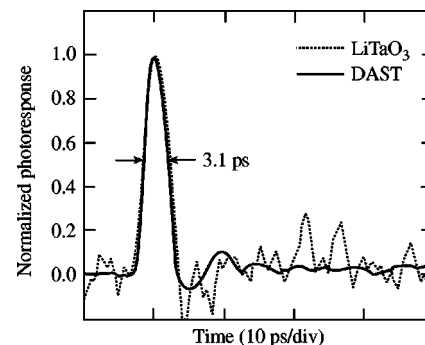


FIG. 2. Comparison between the photoresponse transients measured under the same experimental conditions using the DAST and LiTaO<sub>3</sub> transducers.

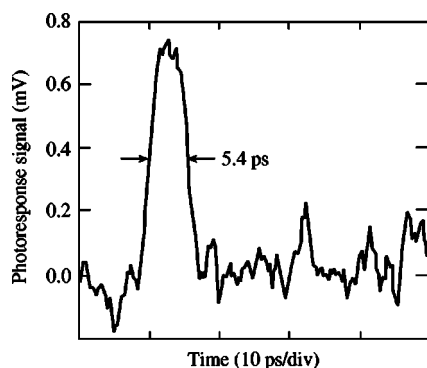


FIG. 3. Submillivolt-amplitude signal recorded using our DAST-based EO sampling system. The presented signal was averaged 30 times in order to reduce the noise level to below  $20 \mu\text{V}$ .

Figure 2 shows the photoreponse signal (solid line) generated by the MSM diode and recorded with the DAST sensor at a spot approximately  $200 \mu\text{m}$  away from the diode (see inset in Fig. 1). The MSM diode was dc biased at 8.3 V, and the average excitation power was 2.5 mW. For comparison, the same measurement, under the same experimental conditions, was performed with the standard  $\text{LiTaO}_3$  finger probe transducer;<sup>21</sup> the obtained wave form is shown in Fig. 2 as a dotted line. We note that both signals have an identical, 3.1-ps-wide full width at half maximum (FWHM), which was limited by the capacitive time constant of the interdigitated finger structure of the MSM diode and the signal propagation distance in CPW. At the same time, there is an improvement of over one order of magnitude of the signal-to-noise ratio in the DAST EO transducer.

Figure 3 demonstrates that our DAST-based EO sampling system is capable of measuring submillivolt signals. We intentionally reduced the bias voltage across the MSM photodetector to 1.1 V and the excitation power to below 0.5 mW and, again, under the same conditions, tested our DAST and  $\text{LiTaO}_3$  systems. Using the DAST transducer, after only 30 averages, we obtained a clean, 0.75 mV, and 5.4-ps-FWHM signal, as shown in Fig. 3. Using the  $\text{LiTaO}_3$  crystal as the EO sensor, even after more than 100 averages (over an hour of averaging time) and additional efforts to reduce the noise, we still could not resolve the submillivolt signal.

Finally, by measuring the propagation evolution of the photoreponse transient along the CPW with the DAST superstrate we could measure the group velocity of  $\sim 1.1 \times 10^8$  m/s and determine the effective dielectric constant as 7.6, which is very close to the quasistatic value, given as the arithmetic average between  $\epsilon_{\text{DAST}} = \epsilon_a = 5.2$  and  $\epsilon_{\text{MgO}} \approx 9.7$ . The latter demonstrates very good coupling of the propagating electrical field into the DAST sensor.

In summary, the DAST single crystal was implemented as a sensor in our room-temperature EO sampling system. As compared to the best  $\text{LiTaO}_3$  sensor, the DAST transducer,

while demonstrating the same time resolution, exhibited a significantly improved electric-field coupling and resulted in measurements with an excellent signal-to-noise ratio. The submillivolt sensitivity and picosecond time resolution of the DAST-based EO samplers, make them practical for characterization of very-high-speed, very-low-power electronic circuits. Using a suitable light source, the DAST can be used to test Si, GaAs, or other semiconductor devices, which are opaque at the wavelength that we used in this work.

The authors thank Carlo Williams for many valuable discussions. This work was supported by the NSF Grant Nos. DMR-0073366 and INT-0078949 and by Corning Inc. One of the authors (S.W.) acknowledges support from the Frank Horton Graduate Fellowship Program in Laser Energetics.

- <sup>1</sup>S. R. Marder, J. W. Perry, and W. P. Schaefer, *Science* **245**, 626 (1989).
- <sup>2</sup>C. P. Yakymyshyn, K. R. Stewart, E. P. Boden, S. R. Marder, J. W. Perry, and P. Schaefer, *Proceedings of the Second International Symposium on Organic Materials for Non-linear Optics* (Royal Society of Chemistry, Cambridge, U.K., 1991), p. 108.
- <sup>3</sup>G. Knöfple, R. Schlessler, R. Ducret, and P. Günter, *Nonlinear Opt.* **9**, 143 (1995).
- <sup>4</sup>F. Pan, G. Knöfple, Ch. Bosshard, S. Follonier, R. Spreiter, M. S. Wong, and P. Günter, *Appl. Phys. Lett.* **69**, 13 (1996).
- <sup>5</sup>Ch. Bosshard, R. Spreiter, and P. Günter, *J. Opt. Soc. Am. B* **18**, 1620 (2001).
- <sup>6</sup>R. Spreiter, Ch. Bosshard, and P. Günter, *Opt. Lett.* **22**, 564 (1997).
- <sup>7</sup>X.-C. Zhang, X. F. Ma, Y. Jin, T.-M. Lu, and E. P. Boden, *Appl. Phys. Lett.* **61**, 3080 (1992).
- <sup>8</sup>K. Kawase, M. Mizuno, S. Sohma, H. Takahashi, T. Taniuchi, and H. Ito, *Opt. Lett.* **24**, 1065 (1999).
- <sup>9</sup>T. J. Carrig, G. Rodriguez, T. S. Clement, A. J. Taylor, and K. R. Stewart, *Appl. Phys. Lett.* **66**, 121 (1995).
- <sup>10</sup>T. J. Carrig, G. Rodriguez, T. S. Clement, A. J. Taylor, and K. R. Stewart, *Appl. Phys. Lett.* **66**, 10 (1995).
- <sup>11</sup>P. Y. Han, M. Tani, F. Pan, and X.-C. Zhang, *Opt. Lett.* **25**, 675 (2000).
- <sup>12</sup>M. S. Litz, D. C. Judy, G. A. Huttlin, C. Lazard, L. F. Libelo, X.-C. Zhang, and Z. Lu, *Proc. SPIE* **3158**, 72 (1997).
- <sup>13</sup>M. Thakur, J. Xu, A. Bhowmik, and L. Zhou, *Appl. Phys. Lett.* **74**, 635 (1999).
- <sup>14</sup>F. Pan, K. McCallion, and M. Chiappetta, *Appl. Phys. Lett.* **74**, 492 (1999).
- <sup>15</sup>B. Cai, T. Hattori, H. H. Deng, K. Komatsu, C. Zawadzki, N. Keil, and T. Kaino, *Jpn. J. Appl. Phys.* **40**, L964 (2001).
- <sup>16</sup>U. Meiner, M. Bösch, Ch. Bosshard, F. Pan, and P. Günter, *J. Appl. Phys.* **83**, 3486 (1998).
- <sup>17</sup>N. A. van Dantzig, P. C. M. Planken, and H. J. Bakker, *Opt. Lett.* **23**, 466 (1998).
- <sup>18</sup>S. R. Forrest, P. E. Burrows, A. Stroustrup, D. Strickland, and V. S. Ban, *Appl. Phys. Lett.* **68**, 1326 (1996).
- <sup>19</sup>F. Pan, M. S. Wong, Ch. Bosshard, and P. Günter, *Adv. Mater.* **8**, 592 (1996).
- <sup>20</sup>J. A. Valdmanis, G. Mourou, and C. W. Gabel, *Appl. Phys. Lett.* **41**, 211 (1982).
- <sup>21</sup>X. Zheng, S. Wu, R. Adam, M. Mikulics, A. Förster, J. Schelten, M. Siegel, P. Kordos, and R. Sobolewski, *Proc. SPIE* **5123**, 69 (2003).
- <sup>22</sup>Rainbow Photonics, Einsteinstrasse, HPF E15.2, CH-8093 Zürich, Switzerland; <http://www.rainbowphotonics.ethz.ch>
- <sup>23</sup>R. Adam, M. Mikulics, A. Förster, J. Schelten, M. Siegel, P. Kordos, X. Zheng, S. Wu, and R. Sobolewski, *Appl. Phys. Lett.* **81**, 3485 (2002).